Use of PML Absorbing Layers for the Truncation of the Head Model in Cellular Telephone Simulations

Gianluca Lazzi, *Senior Member, IEEE*, Om P. Gandhi, *Life Fellow, IEEE*, and Dennis M. Sullivan, *Senior Member, IEEE*

***Abstract*—An efficient implementation of the perfectly matched layer (PML) boundary has been used to truncate a 3-mm resolution head model used for cellular telephone simulations. An extensive analysis of the model truncation effects along all three axes has been performed. A basic observation is that a considerable fraction of the power radiated by a cellular telephone is absorbed in the proximal ear region, and there is no interest for safety certification and antenna design in retaining electromagnetic-field information in the weakly exposed regions. We have progressively reduced the finite-difference time-domain space in the ear-to-ear, back-to-front, and bottom-to-top directions by embedding the weakly exposed sides of the head in the PML layers. Results show that, at the lower frequency of 835 MHz, only truncations in the ear-to-ear direction is appropriate for specific-absorption-rate (SAR) accuracy. However, at the personal communication system frequency of 1900 MHz, 1- and 10-g SARs within 1% of accuracy can be obtained by retaining just 4% of the original volume of the head model. This method indicates that high-resolution cellular telephone simulations can be performed with tremendous savings in execution times and memory requirements. All of the SAR results presented in this paper have been obtained with a laptop computer, and execution times as low as 1 min have been obtained for the fully optimized simulations at 1900 MHz. Furthermore, it is shown that by using a truncated half-model, it is possible to obtain accurate radiation patterns at both frequencies of 835 and 1900 MHz. Since both the SAR evaluation and radiation pattern calculation are needed for new antenna design, this should result in a highly efficient algorithm for electromagnetic design of new personal wireless devices.**

***Index Terms*—Cellular telephone, dosimetry, electromagnetic-field effects, FDTD methods.**

I. Introduction

NUMERICAL simulations are routinely used to determine whether cellular telephones comply with current American National Standards Institute (ANSI)/IEEE safety standards [1]. Recently, the Federal Communications Commission (FCC) has started to require that every new cellular telephone be tested for compliance with the FCC Safety Guidelines [2].

The finite-difference time-domain (FDTD) method [3]–[5] is the preferred numerical technique for cellular telephone simulations since it allows the inclusion of arbitrarily heterogeneous objects in the region to be simulated. Therefore, several authors have developed and successfully used highly realistic heterogeneous human head models for cellular telephone simulations [6]–[10]. These models are characterized by resolutions as low as 1 mm, and as many as 32 tissue types have been identified. Moreover, computer-aided design (CAD) files such as Pro-Engineer have been used to improve the realism in the modeling of the device [11], [12].

The major drawbacks of these simulations are the execution time and computer memory requirements. Several authors have proposed methods to reduce memory requirements, or execution times, or both, but all the presented methods need special modifications of the computer code.

Okoniewski *et al.* [13] introduced a subgridding method suitable for representing with high resolution the regions of maximum absorption, and lower resolution the regions where the electromagnetic coupling is weak. In this approach, the major drawback is the need to implement the subgridding scheme in the FDTD code. Therefore, while the method is extremely useful in cases where is necessary to model the entire domain, for cellular telephone certification, it is not extremely handy since the real interest for compliance testing is only in the 1- and 10-g average specific absorption rates (SARs) of power.

Lazzi and Gandhi [9] have previously developed a truncation scheme that requires minimal modifications to any FDTD codes, and it performs well. The drawback of this method, however, is the need to run two simulations in sequence to obtain exact results in the entire modeled region. Moreover, since the method uses symmetry principles, the head model can be truncated only in the ear-to-ear direction.

Tinniswood *et al.* [12] introduced an expanding grid method for accurate modeling of the region of interest (ear) and increasingly coarser modeling of the weakly exposed regions of the human head. The method is very efficient, but it still requires the uncoupled regions to be retained. It can be combined with the truncation method presented in [9], but, once again, because of the symmetry requirement, the head model can only be truncated in the ear-to-ear direction.

In this paper, we investigate the use of the perfectly matched layer (PML) absorbing layers [14] for the purpose of truncating the head model. The unsplit step formulation in [15] has been implemented, and the possibility of truncating the head model in all the directions has been carefully considered. The implemented absorbing boundary conditions (ABCs) allowed truncation in the ear-to-ear direction (x), back-to-front direction (y), and bottom-to-top direction (z), thereby leaving just a small percentage of the volume of the original head model for simulation. No reflections from the interfaces between the head model and the absorbing PML layers have been observed. While at the lower frequency of 835 MHz, truncations other than in the

Manuscript received December 10, 1999; revised March 1, 2000.

G. Lazzi is with the Department of Electrical and Computer Engineering, North Carolina State University, Raleigh, NC 27695-7914 USA.

O. P. Gandhi is with the Department of Electrical Engineering, University of Utah, Salt Lake City, UT 84112 USA.

D. M. Sullivan is with the Department of Electrical Engineering, University of Idaho, Moscow, ID 83843 USA.

Publisher Item Identifier S 0018-9480(00)09694-0.

ear-to-ear direction did not provide extremely accurate results, at 1900 MHz, just a small volume beyond the ear region was found to be adequate to obtain accurate results for SAR distributions and peak 1- and 10-g SARs.

This allowed us to perform the simulations on a laptop computer equipped with a Pentium II processor, obtaining outstanding performance for both execution times and memory usage.

Furthermore, it is shown that by using only a half-truncated head model it is possible to achieve accurate radiation patterns at both 835 and 1900 MHz. Therefore, when a complete characterization of the handset performance is needed, it is possible to use the proposed approach with a considerable saving for SAR evaluation and a more limited saving for radiation pattern calculation in both execution time and memory requirements.

II. FDTD Implementation and Head Model

The FDTD code needs to be implemented slightly differently to account for the PML layers according to the formulation presented in [15]. In fact, instead of calculating only the electric (**E**) and magnetic (**H**) fields as in the simplest FDTD scheme, in this formulation, the electric displacement field **D** must also be computed. Therefore, there is a slight general increase of memory usage (due to three additional arrays corresponding to the three components of the **D** field that must be stored and additional matrices necessary in the PML region) and execution time (three additional components that need to be calculated). However, the advantages are the outstanding performance of the PML boundary conditions and the possibility of terminating without reflections any materials. This formulation is basically equivalent to that proposed by Gedney [16], which presents an anisotropic PML for the FDTD method that uses the classical **E** and **H** update scheme.

The implementation of the PML with **D** and **H** fields has the advantage of making the PML completely independent to the background medium, and separate from any real conductivity in the FDTD domain. Moreover, frequency-dependent properties can be assigned with minimal modifications to the code. The method can be implemented by adding fictitious dielectric constants and permeabilities ε^*_{Fm} and μ^*_{Fm} that are not related to the real values of ε^*_r used for specifying the materials in the FDTD space. Following closely the theory in [15], and taking into account the conditions on the fictitious dielectric constants given in [17], the D_z-field component can be derived, for example, from the following equation:

$$j\omega\left(1+\frac{\sigma_x(x)}{j\omega\varepsilon_0}\right)\left(1+\frac{\sigma_y(y)}{j\omega\varepsilon_0}\right)\left(1+\frac{\sigma_z(z)}{j\omega\varepsilon_0}\right)^{-1}D_z = c_0\left(\frac{\partial H_y}{\partial x}-\frac{\partial H_x}{\partial y}\right) \quad (1)$$

where σ_m ($m = x$, y, or z) are fictitious conductivities. Equation (1) can be rewritten as

$$j\omega\left(1+\frac{\sigma_x(x)}{j\omega\varepsilon_0}\right)\left(1+\frac{\sigma_y(y)}{j\omega\varepsilon_0}\right)D_z = c_0\left(\mathrm{curl\_}h+\frac{\sigma_z(z)}{\varepsilon_0}I_{Dz}\right) \quad (2)$$

with

$$\mathrm{curl\_}h = \left(\frac{\partial H_y}{\partial x}-\frac{\partial H)x}{\partial y}\right) \quad (3)$$

and

$$I_{Dz} = \frac{1}{j\omega}\,\mathrm{curl\_}h \quad (4)$$

which is an integration in the time domain.

In finite-difference formulation, (2)–(4) can be written as follows:

$$\begin{aligned}\mathrm{curl\_}h = {} & H^{n-1/2}(i+1/2,j,k+1/2) \\ & - H_y^{n-1/2}(i-1/2,j,k+1/2) \\ & + H_x^{n-1/2}(i,j+1/2,k+1/2) \\ & - H_x^{n-1/2}(i,j+1/2,k+1/2)\end{aligned} \quad (5)$$

$$I^n_{Dz}(i,j,k+1/2) = I^{n-1}_{Dz}(i,k,k+1/2)+\mathrm{curl\_}h \quad (6)$$

$$\begin{aligned}D^n_z(i,j,k+1/2) = {} & gi3(i)\cdot gj3(j)\cdot D^{n-1}_z(i,j,k+1/2) \\ & + gi2(i)\cdot gj2(j)\cdot 0.5\cdot\big(\mathrm{curl\_}h+gk1(k) \\ & \cdot I^n_{Dz}(i,j,k+1/2)\big)\end{aligned} \quad (7)$$

where the coefficients g are defined as

$$\begin{aligned}gk1(k) &= xn(k) \\ gi2(i) &= 1/\big(1+xn(i)\big) \\ gj2(j) &= 1/\big(1+xn(j)\big) \\ gi3(i) &= \big(1-xn(i)\big)/\big(1+xn(i)\big) \\ gj3(j) &= \big(1-xn(j)\big)/\big(1+xn(j)\big).\end{aligned} \quad (8)$$

In (8), xn has been found empirically and it is given by

$$xn(m) = .333\cdot\left(\frac{m}{\text{No. PML layers}}\right)^3 \qquad m = 1,\ldots,\text{No. PML layers}. \quad (9)$$

Similar equations can be derived for all the other field components.

The 1- and 10-g SARs have been calculated with a post-processing routine. The algorithm scans each cell of the model and expands in the shape of a cube around the considered cell. Boundaries of the head model are identified so that the 1- or 10-g cubes are within the head model, in the sense that each face of the cube contains at least one cell of the model.

The input power has been calculated by using the discrete Fourier transform (DFT) of the input voltage and current, and the obtained value is compared with the sum of radiated and absorbed power to assure for the convergence of the code.

The head model has been derived from a 2 × 2 × 3 mm resolution anatomically based model, obtained from the magnetic resonance imaging (MRI) scans of a male volunteer. The original whole-body model described in [6] has been classified into 31 tissue types, 16 of which are present in the human head model. The dielectric properties used for the various classified tissues are the same as reported in [6]. To simplify the present calculations, the model has been resampled with a resolution of 3 mm^3, which is still adequate for SAR calculations at the

cellular telephone frequencies of 835 and 1900 MHz. The resampling algorithm first subdivides the model to a resolution of 1 mm, and then it groups 27 cells at the time to create the 3-mm resolution model by majority of the tissues present in each subvolume of 27 cells.

Another anatomically based model with a resolution of less than 1 mm is also available [11], but it has not been used for the purpose of illustrating the present truncation method.

III. Description of the Considered Cases

First, the complete head model simulation has been run to obtain the correct results at the irradiation frequencies of 835 and 1900 MHz, typical of today's cellular telephones. For the purpose of this paper, the telephones have been modeled by using a plastic-covered metal box of dimensions $2.4 \times 5.4 \times 15$ cm equipped with a $\lambda/4$ antenna. The plastic cover is 3-mm thick and its electrical properties are $\varepsilon_r = 1.6, \sigma = 0$. The antenna has been placed on the top of the telephone at a distance of 3 mm from the distal surface and 3 mm from the front side. To understand the capability of the PML layers to terminate the head model, we have progressively limited the FDTD space in the ear-to-ear direction (x-direction) by gradually immersing the uncoupled side of the head into the PML layers. Later, we have gradually reduced the back to front size of the FDTD space (y-direction) by progressively immersing the back and the nose and eyes of the head model into the absorbing layers. Lastly, in some cases, we have reduced the bottom-to-top size of the FDTD space (z-direction) by removing as many layers as permitted by the physical extent of the antenna from the top of the head model. This has been possible due to the particular implementation of the PML boundaries that allows immersing parts of the head model into the absorbing layers, regardless of their dielectric constants.

In this way, we have progressively reduced the x-direction of the head model from 69 to 19 cells (73% reduction) and in the y-direction from 76 to 30 cells (61% reduction). However, since we have used a six-layer PML boundary, the actual number of cells used for the SAR computation is 13 in the x-direction ($19 - 6$, 81% reduction) and 18 in the y-direction ($30 - 6 - 6$, 76% reduction). The z-direction has been reduced by 0%–18%, depending upon the length of the antenna.

Overall, the original head model composed by 445 740 cubical cells has been progressively reduced down to a minimum of 39 900 cells model, corresponding to a volume saving of approximately 91%. Considering, as mentioned above, that six cells of the head model in the x-direction and 12 cells of the head model in the y-direction were actually unused in the SAR computation since they were immersed in the PML layers, the actual numbers of cells for the truncated head model is as low as 16 380. This corresponds to a reduction in the volume of the head model by as much as 96%.

IV. SAR Results

Tables I and II show the actual 1-g average SARs values obtained at the two considered frequencies of 1900 and 835 MHz, respectively, for some of the considered truncated models. The radiated power is 125 mW at 1900 MHz and 600 mW at 835 MHz, and the antenna length is $\lambda/4$ in both cases. We also give in the same table the truncation percentage in the x- and y-directions, as well as the nomenclature used to identify each of the truncated models. We will refer in some of the presented results as relative to models identified by two letters, related to the x- and y-truncations, respectively. For example, according to the nomenclature used in Tables I and II, the model "AB" refers to a model truncated by 67% in the x-direction and 37% in the y-direction, respectively.

TABLE I
1-g Average SARs in Watts per Kilogram for the Human Head Model for the Assumed Cellular Telephone Using a $\lambda/4$ Antenna. Frequency = 1900 MHz. Radiated Power = 125 mW. Truncation for the x-Direction Alone Gives a Maximum Error of 0.6%. The Maximum Error for All the Considered Cases is 0.8%

		% Truncation in the Ear-to-Ear (x) direction			
		0 % (Full)	67 % (A)	74 % (B)	81 % (C)
% Truncation in the Back to Front (y) direction	0 % (Full)	**1.114**	1.114	1.107	1.109
	24 % (A)	-	1.114	1.111	1.109
	37 % (B)	-	1.123	1.120	1.117
	61 % (C)	-	1.118	1.116	1.116

TABLE II
1-g Average SARs in Watts per Kilogram for the Human Head Model for the Assumed Cellular Telephone Using a $\lambda/4$ Antenna. Frequency = 835 MHz. Radiated Power = 600 mW. Truncation for the x-Direction Alone Gives a Maximum Error of 1.6%. The Maximum Error for All the Considered Cases is 22%. The Maximum Errors are Obtained for Models C for the y-Direction (61% Truncation in the y-Direction)

		% Truncation in the Ear-to-Ear (x) direction			
		0 % (Full)	67 % (A)	74 % (B)	81 % (C)
% Truncation in the Back to Front (y) direction	0 % (Full)	**2.490**	2.530	2.492	2.506
	24 % (A)	-	2.491	2.503	2.490
	37 % (B)	-	2.245	2.213	2.230
	61 % (C)	-	1.950	1.970	2.003

As shown, at the lower frequency of 835 MHz, truncations of the head model in the y-direction (back-to-front) that exceed 30% causes the error to increase considerably. In this case, results accurate to within 1% have been obtained for all the considered truncation in the x-direction (ear-to-ear direction), down to retain only 19% of the head model. However, truncations in the y-direction give progressively increasing error (up to 22%) at the frequency of 835 MHz, which suggests that, for this frequency, it is not desirable to truncate the head model by more than 30% in the y-direction. We attribute this to the fact that, at this frequency, the actual shape of the head in proximity to the ear region affects the radiation from the cellular telephone and its radiated power.

Remarkably, at the higher frequency of 1900 MHz, truncation in both x- and y-directions resulted in extremely accurate results since the absorbed power is extremely concentrated in the ear region and a very small volume behind it. Truncations up to 81%

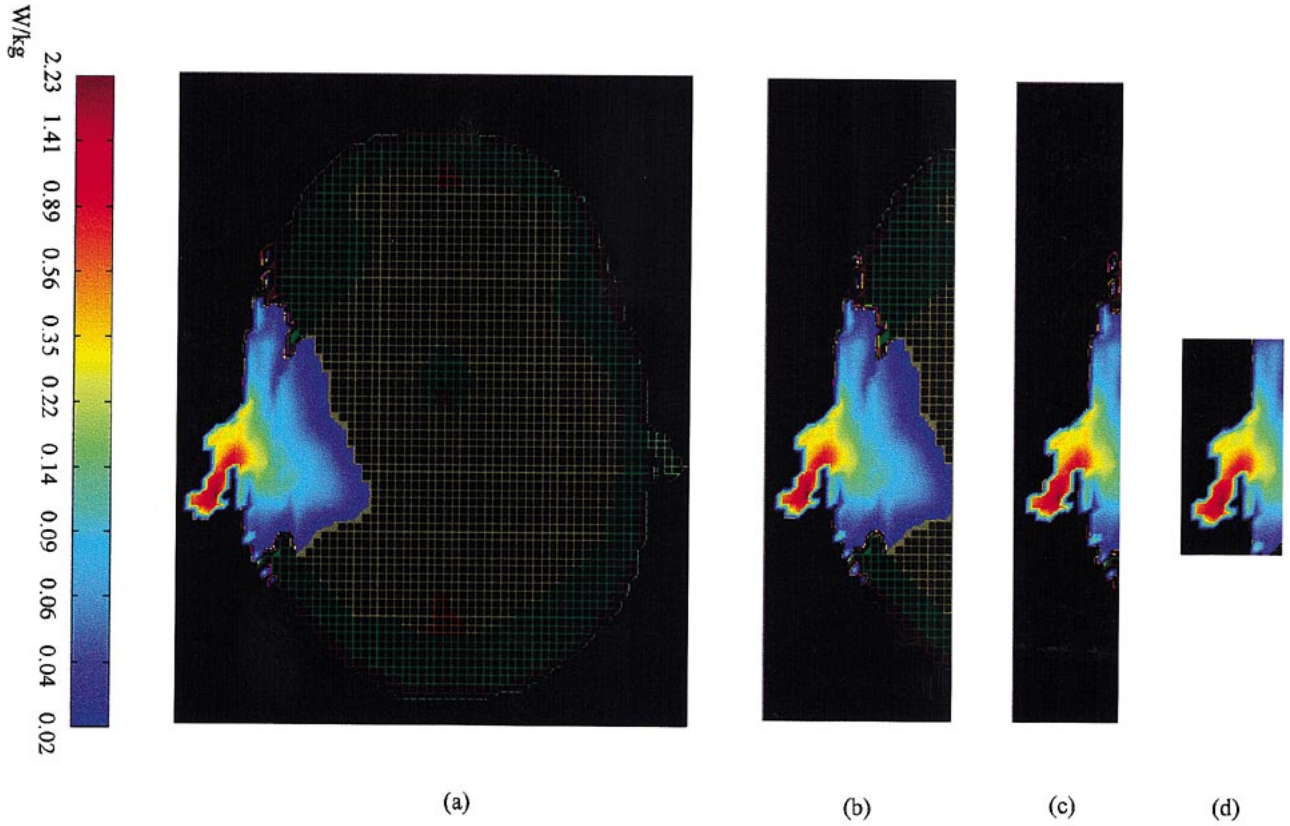

Fig. 1. x–y cross section of the SAR distribution in the human head model for the: (a) full model and truncated models: (b) "Af," (c) "Cf," and (d) "CC" at the frequency of 1900 MHz for a layer that is 6 mm below the antenna feed-point.

TABLE III
10-g AVERAGE SARs IN WATTS PER KILOGRAM FOR THE HUMAN HEAD MODEL FOR THE ASSUMED CELLULAR TELEPHONE USING A $\lambda/4$ ANTENNA. FREQUENCY = 1900 MHz. RADIATED POWER = 125 mW. TRUNCATION FOR THE x-DIRECTION ALONE GIVES A MAXIMUM ERROR OF 0.4%. THE MAXIMUM ERROR FOR ALL THE CONSIDERED CASES IS 1.5%

		% Truncation in the Ear-to-Ear (x) direction			
		0 % (Full)	67 % (A)	74 % (B)	81 % (C)
% Truncation in the Back to Front (y) direction	0 % (Full)	**0.507**	0.506	0.506	0.505
	24 % (A)	-	0.508	0.511	0.507
	37 % (B)	-	0.513	0.515	0.512
	61 % (C)	-	0.514	0.514	0.512

TABLE IV
10-g AVERAGE SARs IN WATTS PER KILOGRAM FOR THE HUMAN HEAD MODEL FOR THE ASSUMED CELLULAR TELEPHONE USING A $\lambda/4$ ANTENNA. FREQUENCY = 835 MHz. RADIATED POWER = 600 mW. TRUNCATION FOR THE x-DIRECTION ALONE GIVES A MAXIMUM ERROR OF 1.9%. THE MAXIMUM ERROR FOR ALL THE CONSIDERED CASES IS 18%. THE MAXIMUM ERRORS ARE OBTAINED FOR MODELS C FOR THE y-DIRECTION (61% TRUNCATION IN THE y-DIRECTION)

		% Truncation in the Ear-to-Ear (x) direction			
		0 % (Full)	67 % (A)	74 % (B)	81 % (C)
% Truncation in the Back to Front (y) direction	0 % (Full)	**1.400**	1.407	1.397	1.427
	24 % (A)	-	1.408	1.404	1.413
	37 % (B)	-	1.292	1.270	1.285
	61 % (C)	-	1.148	1.155	1.170

in the x-direction and up to 76% in the y-direction did not affect the accuracy of the results for the 1-g SARs. Tables III and IV show the 10-g average SARs for the same set of 12 truncated head models. Accuracies similar to those of Tables I and II have been obtained in these cases as well.

Fig. 1 shows an x–y cross section of the SAR distribution in the human head model for the full model [see Fig. 1(a)] and truncated models [see Fig. 1(b)–(d)] at the frequency of 1900 MHz for a layer that is 6 mm below the antenna feed point. The truncated models are, respectively: "Af" [67% truncation in the x-direction and 0% in the y-direction, Fig. 2(b)], "Cf" [81% truncation in the x-direction and 0% in the y-direction, Fig. 2(c)], and "CC" [81% truncation in the x-direction and 61% in the y-direction, Fig. 2(d)]. As shown, the agreement of the SAR distributions between the truncated models and the full model is excellent. Results are shown in logarithmic scale so that even the smallest SAR values near the truncation boundaries may also be shown. It is possible to observe that virtually no reflection arises from either truncation, in the x- or y-directions.

Figs. 2 and 3 show the SAR variations for lines parallel to the x-axis passing through the two ears at the feed-point elevation and 6 mm below the feed point, respectively for the four models considered in Fig. 1 ("Full," "Af," "Cf," and "CC"). Both SAR

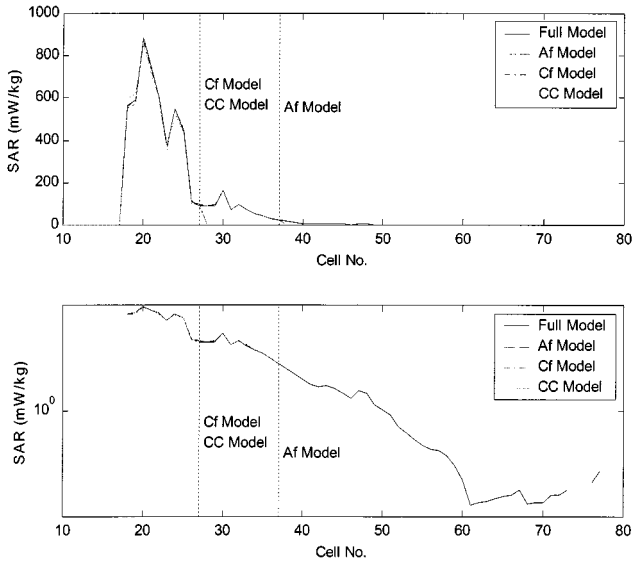

Fig. 2. SAR distributions on an imaginary line passing from ear to ear at the feed-point elevation for the four models considered in Fig. 2 ("Full," "Af," "Cf," and "CC"). (a) Linear scale. (b) Logarithmic scale.

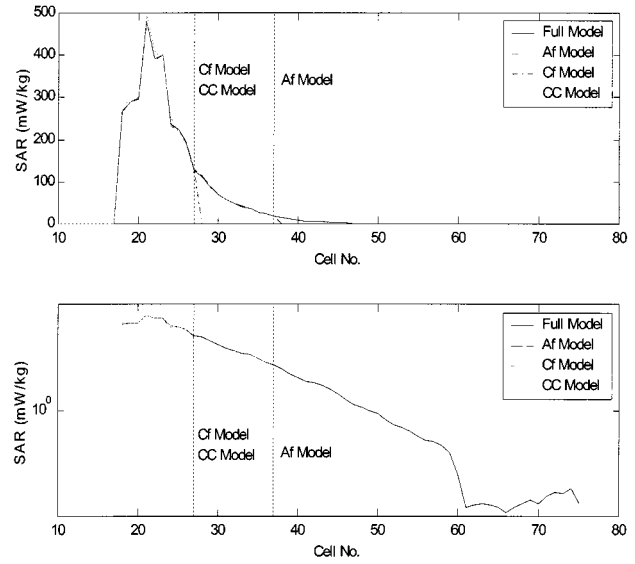

Fig. 3. SAR distributions on an imaginary line passing from ear to ear 6 mm below the feed point for the four models considered in Fig. 2 ("Full," "Af," "Cf," and "CC"). (a) Linear scale. (b) Logarithmic scale.

lines are shown in linear and logarithmic scales so that both the accuracy of the peak values and the details can be observed. As shown, the accuracy of the results for the various truncated head models is excellent. The accuracy of the SARs in all the points of the truncated models is also evident from Fig. 4, where the SAR for each cell of the models "Af," "Bf," and "Cf," is plotted as a function of the SAR for the full model at the same cell. A perfect straight line at 45° angle would give the perfect agreement of the SAR in every location of the head model, and the considered cases are remarkably close to the ideal case.

Table V shows the performance in terms of memory usage and execution times at the frequency of 1900 MHz for the various truncated models in the x- and y-directions. The simulations have been performed on a laptop computer equipped with

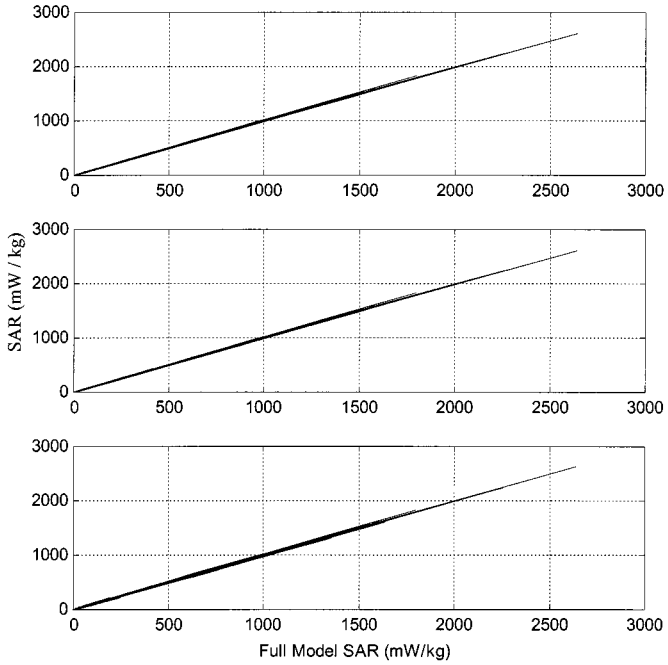

Fig. 4. SAR for each cell of the models "Af," "Bf," and "Cf" plotted as a function of the SAR for the full model at the same cell. (a) "Af": "Full." (b) "Bf": "Full." (c) "Cf": "Full."

TABLE V
MEMORY REQUIREMENTS AND SIMULATION TIMES FOR ALL THE CONSIDERED HEAD MODELS. FREQUENCY = 1900 MHz. SIMULATION TIMES FOR THE 835-MHz FREQUENCY ARE APPROXIMATELY TWICE THESE VALUES. DATA REFERS TO A LAPTOP COMPUTER EQUIPPED WITH A PENTIUM II PROCESSOR

		% Truncation in the Ear-to-Ear (x) direction							
		0 % (Full)		67 % (A)		74 % (B)		81 % (C)	
		Mem. Mb	Time mins.	Mem. Mb	Time mins.	Mem. Mb	Time mins.	Mem. Mb	Time mins.
% Truncation in the Back to Front (y) direction	0 % (Full)	60	16	34	5.3	31	4.6	27	4
	24 % (A)	-	-	27	3.8	24	3.4	22	2.9
	37 % (B)	-	-	23	3.2	21	2.9	19	2.7
	61 % (C)	-	-	17	2.1	15	1.9	13	1.4 *

*: One additional model with truncation by 18% in the z-direction from the top of the head model needed a reduced memory of 11 Mb and an execution time of 1 min.

a Pentium II processor. The savings in both memory and execution times is remarkable. Memory savings on the order of 80% and execution time reduction over 90% are achieved by using the proposed method. At the frequency of 835 MHz, execution times are approximately twice of these values. At the frequency of 1900 MHz, it was possible to also truncate the top of the head model by 18%. This led to a 1-min execution time (94% reduction) and 11-Mb memory usage (82% reduction) for this case, still maintaining the error within 1%.

V. RADIATION PATTERN RESULTS

We have also calculated the radiation pattern in presence of the human head model, and have compared the radiation patterns of the considered cellular telephone in presence of the trun-

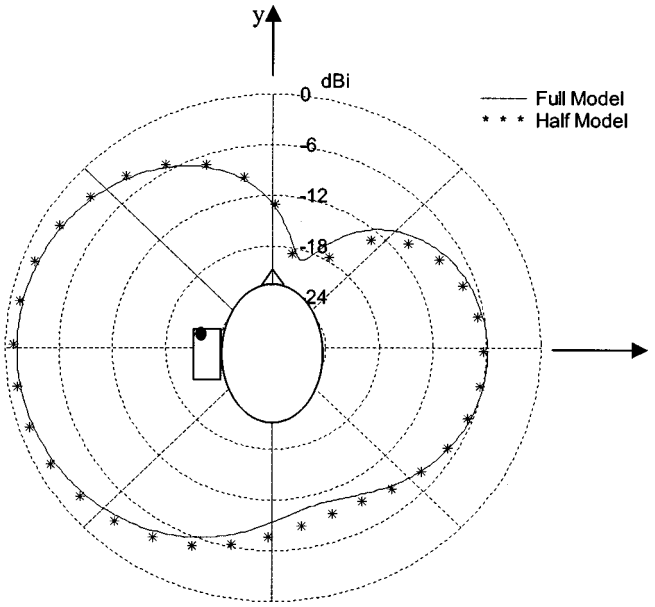

Fig. 5. Radiation patterns for the "full" (line) and "truncated half" (*) models. Frequency: 1900 MHz.

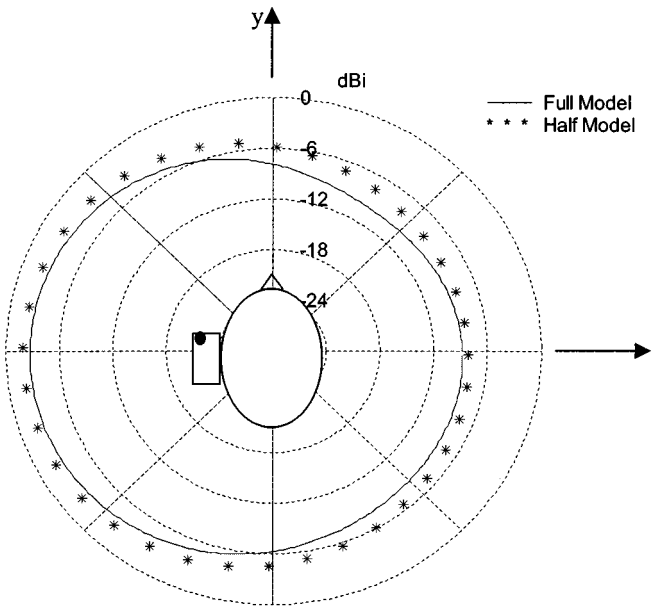

Fig. 6. Radiation patterns for the "full" (line) and "truncated half" (*) models. Frequency: 835 MHz.

cated models and full model. Since a near-to-far-field transformation using the Green's theorem has been implemented, the scattering structure needs to be entirely enclosed in the surfaces of the region used to calculate the equivalent currents. Therefore, for the radiation pattern subroutine, an approximation has been made where the fields calculated in the uncoupled region of the head are considered to be in air. For radiation pattern calculations, this corresponds to have physically terminated head model, while the field components have been calculated in reality by assuming absorbing layers in the missing part of the model rather than air.

By using this method, it is found that no less than a half-truncated model should be used to obtain accurate results. In reality, the use of a half-truncated model corresponds to the actual use of the electromagnetic field only in approximately one-third of the model itself since six cells are used in immersing the head model into the absorbing boundaries, and two cells of distance between boundaries and surfaces for radiation pattern computation have been taken.

Figs. 5 and 6 compare the radiation patterns in the x–y-plane for the full and truncated half-models at the frequency of 1900 and 835 MHz, respectively. As shown, in both cases, the agreement is fairly good. By reducing more of the head model, we have verified that the radiation pattern tends to distort, becoming progressively closer to the free-space radiation pattern.

Execution times for these cases are approximately half of the execution times for the full-model cases.

The approach can be successfully used in the design of new cellular telephone antennas since many simulations, both for SAR and radiation pattern, may be necessary to optimize the designs. While for SAR calculations the savings in execution time and computer memory are substantial, somewhat less saving (on the order of a factor of two) are obtained for radiation pattern simulations.

VI. Conclusions

We have shown that by using a PML ABC it is possible to considerably reduce the size of the FDTD space to be considered for cellular telephone simulations. Different from the previously proposed techniques, this method allows truncation along all three axes. Reductions of the head volume down to 4% of the original volume have been achieved, and memory savings of up to 82% have been obtained. Execution times are consequently no more than 7% of the original values. This approach makes it possible to perform SAR simulations on a commonly available computer as opposed to a high-end workstation generally required to handle the full simulations. When the radiation pattern is also of interest, the truncated half-models provide better accuracy. The method may be used for repetitive simulations needed for optimized designs of antennas and personal wireless devices.

References

[1] *American National Standard—Safety Levels with Respect to Exposure to Radio Frequency Electromagnetic Fields, 3 kHz to 300 GHz*, ANSI/IEEE Standard C95.1–1992, 1992.

[2] "Guidelines for Evaluating the Environmental Effects of Radiofrequency Radiation," Federal Commun. Commission, Washington, DC, FCC Rep. 96–326, Aug. 1996.

[3] A. Taflove, *Computational Electrodynamics: The Finite-Difference Time-Domain Method*. Norwood, MA: Artech House, 1995.

[4] ——, *Advances in Computational Electrodynamics: The Finite-Difference Time-Domain Method*. Norwood, MA: Artech House, 1998.

[5] K. S. Kunz and R. J. Luebbers, *The Finite-Difference Time-Domain Method in Electromagnetics*. Boca Raton, FL: CRC Press, 1993.

[6] O. P. Gandhi, G. Lazzi, and C. M. Furse, "Electromagnetic absorption in the human head and neck at 835 and 1900 MHz," *IEEE Trans. Microwave Theory Tech.*, vol. 44, pp. 1884–1897, Oct. 1996.

[7] M. Okoniewski and M. A. Stuchly, "A study of the handset antenna and human body interaction," *IEEE Trans. Microwave Theory Tech.*, vol. 44, pp. 1855–1864, Oct. 1996.

[8] M. A. Jensen and Y. Rahmat-Samii, "EM interaction of handset antennas and a human in personal communication systems," in *Proc. IEEE*, vol. 83, Jan. 1995, pp. 7–17.

[9] G. Lazzi and O. P. Gandhi, "Realistically tilted and truncated anatomically based models of the human head for dosimetry of mobile telephones," *IEEE Trans. Electromagn. Compat.*, vol. 39, pp. 55–61, Feb. 1997.
[10] P. Bernardi, M. Cavagnaro, and S. Pisa, "Evaluation of the SAR distribution in the human head for cellular phones used in a partially closed environment," *IEEE Trans. Electromagn. Compat.*, vol. 38, pp. 357–366, Aug. 1996.
[11] O. P. Gandhi, G. Lazzi, A. D. Tinniswood, and Q. S. Yu, "Numerical and experimental methods for determination of SAR and radiation patterns of handheld wireless telephones," *Bioelectromagnetics*, vol. 20, pp. 93–101, Mar. 1999.
[12] A. D. Tinniswood, G. Lazzi, and O. P. Gandhi, "The use of expanding grid finite difference time domain techniques for simulation of CAD-derived mobile communication devices," *Microwave Opt. Technol. Lett.*, vol. 22, pp. 21–24, 1999.
[13] M. Okoniewski, E. Okoniewska, and M. A. Stuchly, "Three-dimensional subgridding algorithm for FDTD," *IEEE Trans. Antennas Propagat.*, vol. 45, pp. 422–429, Mar. 1997.
[14] J. P. Berenger, "A perfectly matched layer for the absorption of electromagnetic waves," *J. Comput. Phys.*, vol. 114, pp. 185–200, 1994.
[15] D. Sullivan, "An unsplit step 3–D PML for use with the FDTD method," *IEEE Microwave Guided Wave Lett.*, vol. 7, pp. 184–186, July 1997.
[16] S. Gedney, "An anisotropic perfectly matched layer absorbing medium for the truncation of FDTD lattices," *IEEE Trans. Antennas Propagat.*, vol. 44, pp. 1630–1639, Dec. 1996.
[17] Z. S. Sacks, D. M. Kingsland, R. Lee, and J. F. Lee, "A perfectly matched anisotropic absorber for use as an absorbing boundary condition," *IEEE Trans. Antennas Propagat.*, vol. 43, pp. 1460–1463, Dec. 1995.

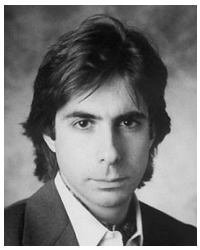

Gianluca Lazzi (S'94–M'95–SM'99) was born in Rome, Italy, on April 25, 1970. He received the Dr.Eng. degree in electronics from the University of Rome "La Sapienza," Rome, Italy, in 1994, and the Ph.D. degree in electrical engineering from the University of Utah, Salt Lake City, in 1998.

He has been a consultant for several companies (1988–1994), Visiting Researcher at the Italian National Board for New Technologies, Energy, and Environment (ENEA) (1994), Visiting Researcher at the University of Rome "La Sapienza" (1994–1995), and Research Associate and Research Assistant Professor at the University of Utah (1995–1998). He is currently an Assistant Professor of electrical and computer engineering at North Carolina State University, Raleigh. He has authored or co-authored over 50 international journal papers or conference presentations on FDTD modeling, wireless antennas, dosimetry, and bioelectromagnetics. He is listed in *Who's Who in the World*, *Who's Who in America*, *Who's Who in Science and Engineering*, *Dictionary of International Biographies*, and *2000 Outstanding Scientists of the 20th Century*.

Dr. Lazzi was the recipient of the 1996 International Union of Radio Science (URSI) Young Scientist Award and the 1996 Curtis Carl Johnson Memorial Award for the best student paper presented at the 18th Annual Technical Meeting of the Bioelectromagnetics Society (BEMS).

Om P. Gandhi (S'57–M'58–SM'65–F'79–LF'99) is currently a Professor and Chairman in the Department of Electrical Engineering, University of Utah, Salt Lake City. He has the authored or co-authored several book chapters and journal papers on electromagnetic dosimetry, microwave tubes, and solid-state devices. He also edited *Biological Effects and Medical Applications of Electromagnetic Energy* (Englewood Cliffs, NJ: Prentice-Hall, 1990) and co-edited *Electromagnetic Biointeraction* (New York: Plenum, 1989). He is listed in *Who's Who in the World*, *Who's Who in America*, *Who's Who in Engineering*, and *Who's Who in Technology Today*.

Dr. Gandhi was the recipient of the 1979–1980 Distinguished Research Award presented by the University of Utah. He has been president of the Bioelectromagnetics Society (1992–1993), co-chairman of the IEEE SCC 28.IV Subcommittee on the RF Safety Standards (1988–1997), and chairman of the IEEE Committee on Man and Radiation (COMAR) (1980–1982). In 1995, he was the recipient of the d'Arsonval Medal of the Bioelectromagnetics Society for pioneering contributions to the field of bioelectromagnetics.

Dennis M. Sullivan (M'89–SM'95) received the Ph.D. degree in electrical engineering from the University of Utah, Salt Lake City, in 1987.

From 1987 to 1993, he was with the Stanford Medical Center, where he developed computerized treatment planning for hyperthermia cancer therapy using the FDTD method. Since then, he has been using the FDTD method for applications such as nonlinear optics, teraherz pulse generation, and quantum semiconductor simulation. He is currently an Associate Professor of electrical engineering at the University of Idaho, Moscow. He authored *Electromagnetic Simulation Using the FDTD Method* (Piscataway, NJ: IEEE Press, 2000).